Journal of Applied Mathematics and Physics, 2020, 8, 1799-1813
https://www.scirp.org/journal/jamp
ISSN Online: 2327-4379
ISSN Print: 2327-4352

Sintering Temperature Dependent Magnetic and Dielectric Properties of Polycrystalline $xBa_{0.95}Sr_{0.05}TiO_3$-$(1-x)BiFe_{0.90}Gd_{0.10}O_3$ Ceramics

M. J. Miah[1*], Mehbuba Rashid Mouri[1], A. Ahad[1], M. A. Taher[1], A. K. M. Akther Hossain[2]

[1]Department of Physics, Comilla University, Cumilla, Bangladesh
[2]Department of Physics, Bangladesh University of Engineering & Technology, Dhaka, Bangladesh
Email: *mmjulhash@yahoo.com

How to cite this paper: Miah, M.J., Mouri, M.R., Ahad, A., Taher, M.A. and Akther Hossain, A.K.M. (2020) Sintering Temperature Dependent Magnetic and Dielectric Properties of Polycrystalline $xBa_{0.95}Sr_{0.05}TiO_3$-$(1-x)BiFe_{0.90}Gd_{0.10}O_3$ Ceramics. *Journal of Applied Mathematics and Physics*, **8**, 1799-1813.
https://doi.org/10.4236/jamp.2020.89135

Received: July 13, 2020
Accepted: September 12, 2020
Published: September 15, 2020

Abstract

Polycrystalline $xBa_{0.95}Sr_{0.05}TiO_3$-$(1-x)BiFe_{0.90}Gd_{0.10}O_3$ ceramics were prepared by standard solid state reaction technique using the solid solution of $BaCO_3$, $SrCO_3$, TiO_2, Bi_2O_3, Fe_2O_3 and Gd_2O_3. The compound is a $BiFeO_3$ based multiferroic material which contains both magnetic and electric properties. The synthesized ceramics noticed better properties than $xBaTiO_3$-$(1-x)BiFeO_3$ because of adding rare earth element Gd which have higher magnetic moment than Fe. The prepared samples were sintered at 900˚C, 950˚C and 1000˚C for 1 h. The effect of sintering temperature on density of the compound, complex initial permeability, dielectric properties and complex impedance analysis was reported in this article. Density of the ceramics was found to be enhanced with the rise in sintering temperature which implied porosity of the compound decreased when sintering temperature was increased. Enhanced complex initial permeability was noticed for the samples up to 950˚C and this might be attributed to reducing the motion of domain wall when the ceramics were sintered above 950˚C. Value of dielectric constant increased whereas dielectric loss decreased and these modifications might be expected because of changing density and grain size due to the variation of sintering temperature. Grain resistance (resistance due to grains) was determined from complex impedance analysis and it reduced with the rise in sintering temperature. The studied multiferroic material exhibited weak ferromagnetism but is an alternative product of environmental hazard lead (Pb) based multiferroic material and it is expected to be environment friendly.

Keywords

Ceramics, Sintering Temperature, Complex Initial Permeability, Dielectric

Properties

1. Introduction

The compounds that consist of metallic and nonmetallic elemental solids are defined as ceramics which are formed by the application of heat and pressure [1]. Generally, ceramic materials have high dielectric strength and high dielectric constant. In comparison to metals, ceramics have very low electrical conductivity due to ionic-covalent bonding which does not form free electrons. Most of the ceramics exhibit ferroelectric behavior. $BaTiO_3$ (BT) is an example of ceramics that have high dielectric constant and it has an enormous application in electronic and solid-state devices such as multilayer capacitors (MLCs), actuators, piezoelectric motor, transducers, filter, resonator, micro-electromechanical system (MEMS) etc. On the other hand, there are several ceramics that exhibit good magnetic properties and ferrites are the example of this kind ceramics. However, nowadays researchers are very much interested to work with the materials having both the electric and magnetic properties simultaneously such as multiferroic materials.

In multiferroic materials electric charges can induce by applying magnetic field and the magnetization can tune by electric field. These materials have immense applications in data storage, spintronics, spin valves, quantum electromagnets and microelectronic devices etc. But these materials are very rare in nature because the criteria for being simultaneously ferroelectric and ferro/antiferromagnetic are mutually restricted. Only a small group of compounds can exhibit both magnetic and electric order parameters simultaneously. Among few known multiferroic materials, perovskite structured $BiFeO_3$ (BFO) is unique, as it exhibits both ferroelectric and antiferromagnetic (weak ferromagnetic) orders simultaneously at and above room temperature. Multiferroic materials might be single-phase or composites. In spite of the room temperature multiferroicity, the incorporation of BFO in practical devices has been restricted because of its several problems. It has high leakage current, large coercive fields and poor electrical insulation etc. However, a lot of researches are running in the world to progress the properties of BFO. To improve magnetic as well as electric properties, recent work has focused on solid solutions of BFO with other perovskites such as $PbTO_3$ (PT), $BaTO_3$ (BT), $SrTiO_3$ (ST), and $Pb(Fe, Nb)O_3$ (PFN) [2] [3] [4] [5]. The solid solution of $xBaTiO_3$-$(1 - x)BiFeO_3$ [BFO-BT] stabilizes the perovskite structure of BFO, contains single phase and exhibits improved multiferroic properties [6]. Previously published article on the studied ceramics $xBa_{0.95}Sr_{0.05}TiO_3$-$(1 - x)BiFe_{0.90}Gd_{0.10}O_3$ [xBST-(1 − x)BFGO] [7] described that the compound has better multiferroic properties than $xBaTiO_3$-$(1 - x)BiFeO_3$ [BFO-BT] and the properties are changed with the variation of BST amount. Here the compound is fabricated changing sintering temperature. The sintering temperature is hoped to play a role in setting the properties of the ceramic samples. An increase in sintering temperature is expected to raise the particle size,

reduce the surface to bulk ratio and have bearings on the grain dependent polarization mechanism. The prepared ceramic samples have been sintered at three different temperatures (900˚C, 950˚C and 1000˚C) to observe the sintering effect on various physical parameters. A detailed study of the effect of sintering temperature on density, complex initial permeability, dielectric properties and impedance characteristics of the material is reported in this article.

2. Experimental Details

2.1. Sample Preparation

Polycrystalline $xBa_{0.95}Sr_{0.05}TiO_3$-$(1-x)BiFe_{0.90}Gd_{0.10}O_3$ [xBST-(1 − x)BFGO] ceramics with x = 0.00, 0.10, 0.20, 0.25, 0.30, 0.35 and 0.40 were fabricated by the conventional solid state reaction technique using the raw materials of $BaCO_3$ (99.9%), $SrCO_3$ (99.9%), TiO_2 (99.9%), Bi_2O_3 (99.9%), Fe_2O_3 (99.9%) and Gd_2O_3 (99.95%). Barium carbonate ($BaCO_3$, 99.9%), Strontium carbonate ($SrCO_3$, 99.9%), Titanium oxide (TiO_2, 99.9%), Bismuth oxide (Bi_2O_3, 99.9%), Ferric oxide (Fe_2O_3, 99.9%) and Gadolinium oxide (Gd_2O_3, 99.95%) powder were purchased from market. The raw materials were mixed in mortar according to the stoichiometric formula. The mixed powders were ball-milled in distilled water for 24 h to obtain homogeneous mixture and then the powders were calcined (pre-sintered) at 850˚C staying in furnace for 1 h. The pre-sintered powders were ground thoroughly and ball-milled again for 12 h for getting a homogeneous mixture. Then 10% polyvinyl alcohol (PVA) was mixed with the powders as a binder for granulation. Disk- and toroid-shaped samples were prepared using the homogeneous mixture by applying a uniaxial pressure of 45 MPa. Dye and hydraulic press were used to make the samples. The green pellets were sintered at various temperatures (900˚C - 1000˚C) in air for 1 h for densification of the samples and to remove moisture. Finally, the samples were polished for characterizing. The sample preparation process is illustrated in the following flowchart:

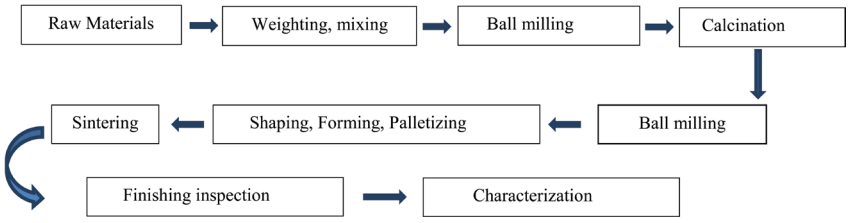

Flow chart of Mixed Oxide route of xBST-(1 − x)BFGO ceramics preparation.

2.2. Characterizations

The crystal structure of the prepared samples was confirmed using X-ray diffractometer (Philips PANalytical X'PERT-PRO) with CuK_α radiation (λ = 1.541 Å) at room temperature. The scanning speed was 1˚ per min in a range of 2θ from 20 to 80˚. The bulk density (ρ_B) of the compositions was calculated using the equation: $\rho_B = \frac{m}{\pi r^2 t}$ where, m is the mass, r is the radius and t is the thickness

of the sample. The value of permeability was measured as a function of frequency within the range of 1 kHz - 100 MHz using a Wayne Kerr 6500B Impedance Analyzer. The value of real part of permeability (μ') was calculated using the relations: $\mu' = \frac{L_S}{L_0}$ and $\tan\delta = \frac{\mu''}{\mu'}$ where, L_s is the self-inductance of the sample core, L_0 is the inductance of the winding of the coil without the sample, μ'' is the imaginary part of permeability and $\tan\delta$ is the magnetic loss. L_0 was determined from geometrical relations, $L_0 = \mu_0 N^2 S/\pi\bar{d}$, where, μ_0 is the permeability in vacuum, N is the number of turns of the coil (N = 5), S is the cross-sectional area and $\bar{d} = (d_1 + d_2)/2$ is the mean diameter of the toroid-shaped sample, d_1 and d_2 are the inner and outer diameter of the toroid-shaped sample respectively. The dielectric measurements were carried out at room temperature within the frequency range of 10 Hz - 10 MHz using Impedance Analyzer. The dielectric constant was determined following the formula: $\varepsilon' = \frac{Ct}{\varepsilon_0 A}$ where, C is the capacitance of the pellet, t indicates the thickness of the pellet, A is the cross-sectional area and ε_0 is the permittivity of free space.

3. Experimental Results

3.1. Structural Study

X-ray diffraction (XRD) patterns of 0.2 BST - 0.8 BFGO ceramics sintered at different temperatures (900˚C, 950˚C and 1000˚C) are shown in Figure 1. X-ray diffraction is one of the important tools to determine the various phases of the synthesized perovskites as well as their unit cell structure. Analyzing the XRD patterns, it is observed that the positions of the peaks comply with the previously reported values [8]. The position of different peaks matches exactly in all the three cases indicating the fact that the variation of sintering temperature does not affect the structural properties of the material. The XRD patterns of all sintered compositions clearly indicate their single phase and formation of simple cubic structure. The lattice constant for each of the sample is calculated using the formula: $a = d\sqrt{h^2 + k^2 + l^2}$ where h, k and l are the Miller indices of the

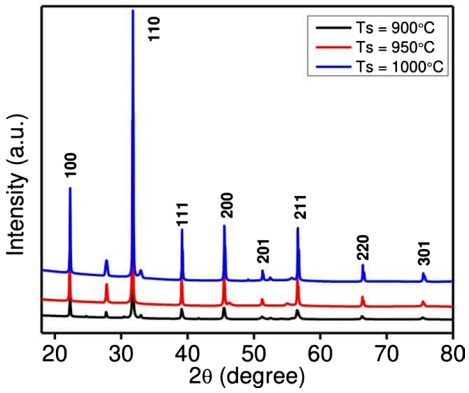

Figure 1. XRD pattern of 0.2 BST - 0.8 BFGO ceramics sintered at 900˚C, 950˚C and 1000˚C temperature.

crystal planes. The value of lattice constant (a) is noticed 3.9710, 3.9850 and 3.9654 and the magnitude of volume of unit cell (V) is found to be 15.77, 15.88 and 15.72 for the samples sintered at 900˚C, 950˚C and 1000˚C respectively.

3.2. Density

The variation of bulk density (ρ_B) of various xBST-(1 − x)BFGO ceramics sintered at 900˚C, 950˚C and 1000˚C staying at 1 h in furnace are shown in **Figure 2**. It is exposed of **Figure 2(a)**, the value of ρ_B decreases with the increase in BST content for all the samples sintered at different temperatures. Decreasing of density with increasing BST content may be due to the incorporation of lower atomic weight BST (230.70 amu) into higher atomic weight BFGO (323.1 amu). Moreover, the substitution of BFGO by BST makes a change in bonding among the elements which causes the change in inter atomic distance and expansion of the unit cell volume and reduces the density [9]. The effect of sintering temperature (T_s) on the change of ρ_B is shown in **Figure 2(b)** and it is seen that ρ_B increases with the increase in sintering temperatures. Samples sintered above 1000˚C became melting and thus the samples were not collected for characterization. The maximum temperature which is tolerable for all the samples is called optimum temperature and better outcomes may be obtained for this temperature. So, all the samples of xBST-(1 − x)BFGO ceramics possess maximum density at 1000˚C means that minimum porosity is available in this temperature.

3.3. Complex Initial Permeability

Permeability means the supportive magnetic field within any material. It is the result of the dynamic response of the magnetic domains due to the applied magnetic field (H) and its value provides information about the inertial position of the domains wall, their arrangement, mutual coupling and spin rotation. Response of the magnetic domains due to low amount applied magnetic field is known as complex initial permeability. Complex initial permeability is the combination of the real part (μ') and imaginary part (μ'') of the permeability of a material. The complex initial permeability is given by, $\mu = \mu' - \mu''$ where, μ' and μ'' is the real and imaginary parts of complex initial permeability, respectively.

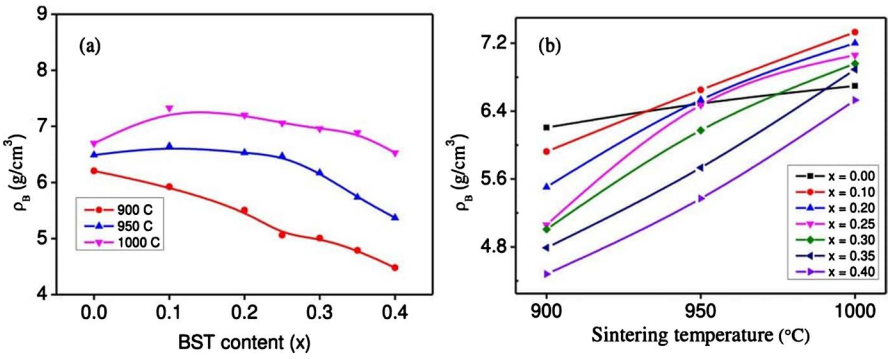

Figure 2. Variation of density with (a) BST content and (b) sintering temperatures of various xBST-(1 − x)BFGO ceramics.

μ' point up the amount of magnetic energy stored in the system which represents the component of magnetic induction B in phase with the applied magnetic field H. On the other hand, μ'' describe the dissipation of magnetic energy which represents the component of magnetic induction B out of phase with H.

Figure 3 shows the variation of μ' with frequency for various xBST-(1 − x) BFGO ceramics sintered at 900˚C, 950˚C and 1000˚C for 1 h. The value of μ' depends on many factors like stoichiometry, composition, grain structure, crystal anisotropy, impurity content, porosity, saturation magnetization, etc. High saturation magnetization, large grain size, low crystal anisotropy, low porosity and high purity of the material are favorable conditions for higher values of permeability [10] [11]. μ' is related to two mechanisms; domain wall motion and spin rotation:

$$\mu' = 1 + \chi_w + \chi_{spin}$$

where, χ_w is the domain wall susceptibility and χ_{spin} is intrinsic rotational

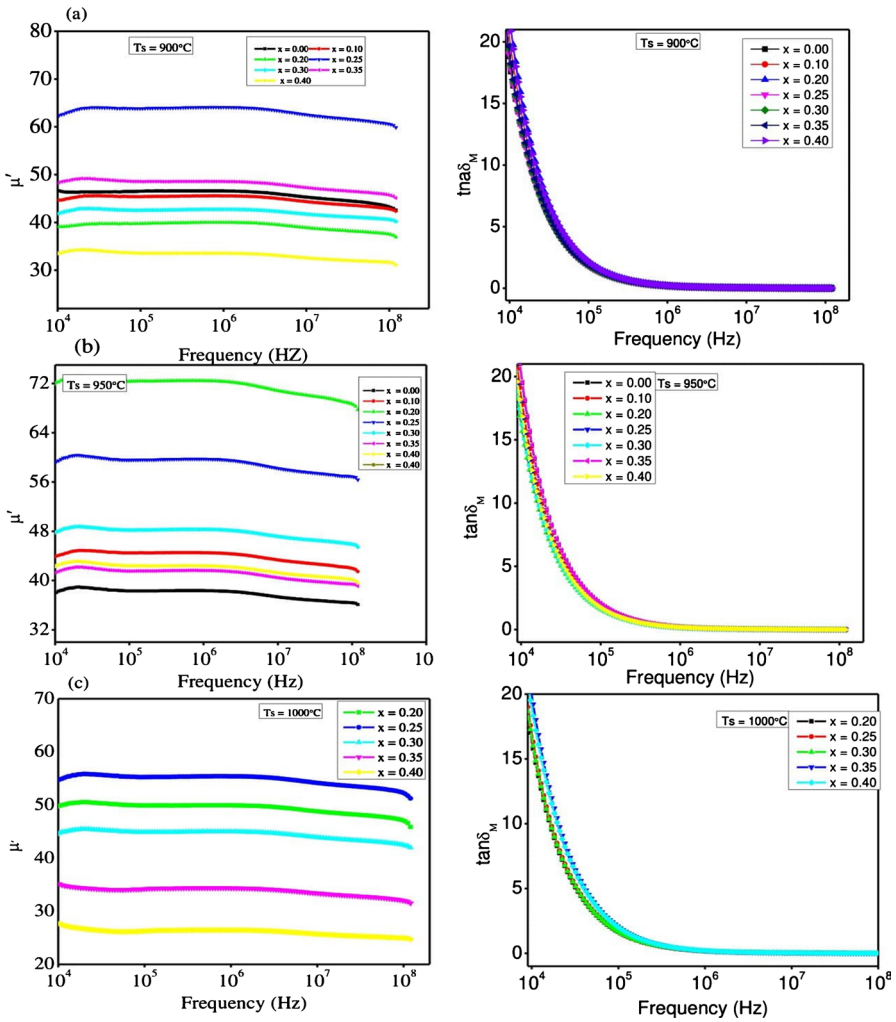

Figure 3. Variation of μ' and $\tan\delta_M$ as a function of frequency of various xBST-(1 − x)BFGO ceramics sintered at (a) 900˚C, (b) 950˚C and (c) 1000˚C for 1 h.

susceptibility. They may be written as $\chi_w = 3\pi M_s^2 D/4\gamma$ and $\chi_{spin} = 2\pi M_s^2/K$ where, M_s is the saturation magnetization, K is the anisotropy constant, D is the average grain diameter, and γ is the domain wall energy [12]. It is noticed that the value of μ' for the samples sintered at different temperatures remains almost constant which represents the frequency stability of μ' for the studied samples. The frequency stability may be responsible for the magnetic moments able to follow the variation of external magnetic field for a longer time during magnetization process [13]. Stability of μ' over a wide range of frequency is a desirable characteristic feature for various applications such as broad band pulse transformers [14] and wide band read-write heads for video recording devices [10] [13]. A slight fall in the values of μ' is observed at higher frequencies for all the samples. This can be explained by the fact that at high frequencies, the unpinning of the domain walls cannot keep motion with the rapidly changing magnetic field which causes diminishing value of μ' [15]. **Figure 3** also represents the variation of magnetic loss ($\tan\delta_M$) (left hand side) as a function of frequency for the samples sintered at three different temperatures. It is seen that $\tan\delta_M$ has maximum value at lower frequency and then decreases exponentially with increasing frequency. The value of $\tan\delta_M$ remains constant after 1 MHz for all the cases. $\tan\delta_M$ arises due to the lag of domain wall motion with respect to the applied field and creates imperfections in the crystal lattice [7].

Variation of μ' and $\tan\delta_M$ with sintering temperatures for various xBST-(1 – x)BFGO ceramics are shown in **Figure 4**. The value of μ' for maximum cases is found to be increased up to 950˚C and then decreases whereas the value of $\tan\delta_M$ is found to be decreased with sintering temperature except for x = 0.35.

3.4. Dielectric Properties

Figure 5 shows the frequency dependence of dielectric constant (ε') and dielectric loss ($\tan\delta_E$) of various xBST-(1 – x)BFGO ceramics sintered at three different temperatures for 1 h. ε' represents the electrical energy stored in materials as

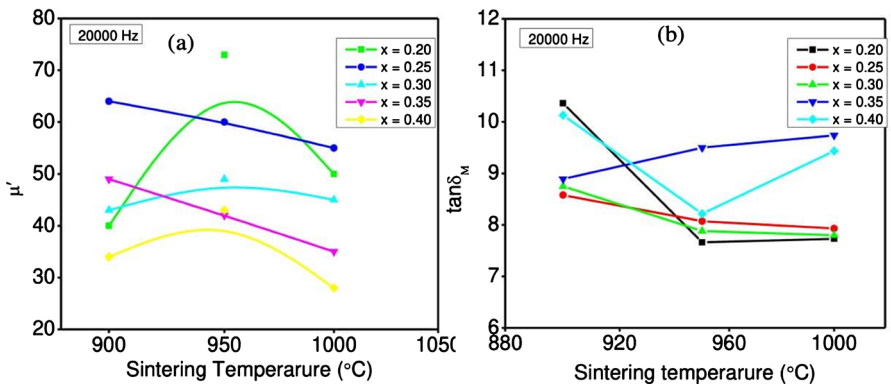

Figure 4. Variation of (a) μ' and (b) $\tan\delta_M$ of various xBST-(1 – x)BFGO ceramics sintered at three different temperatures.

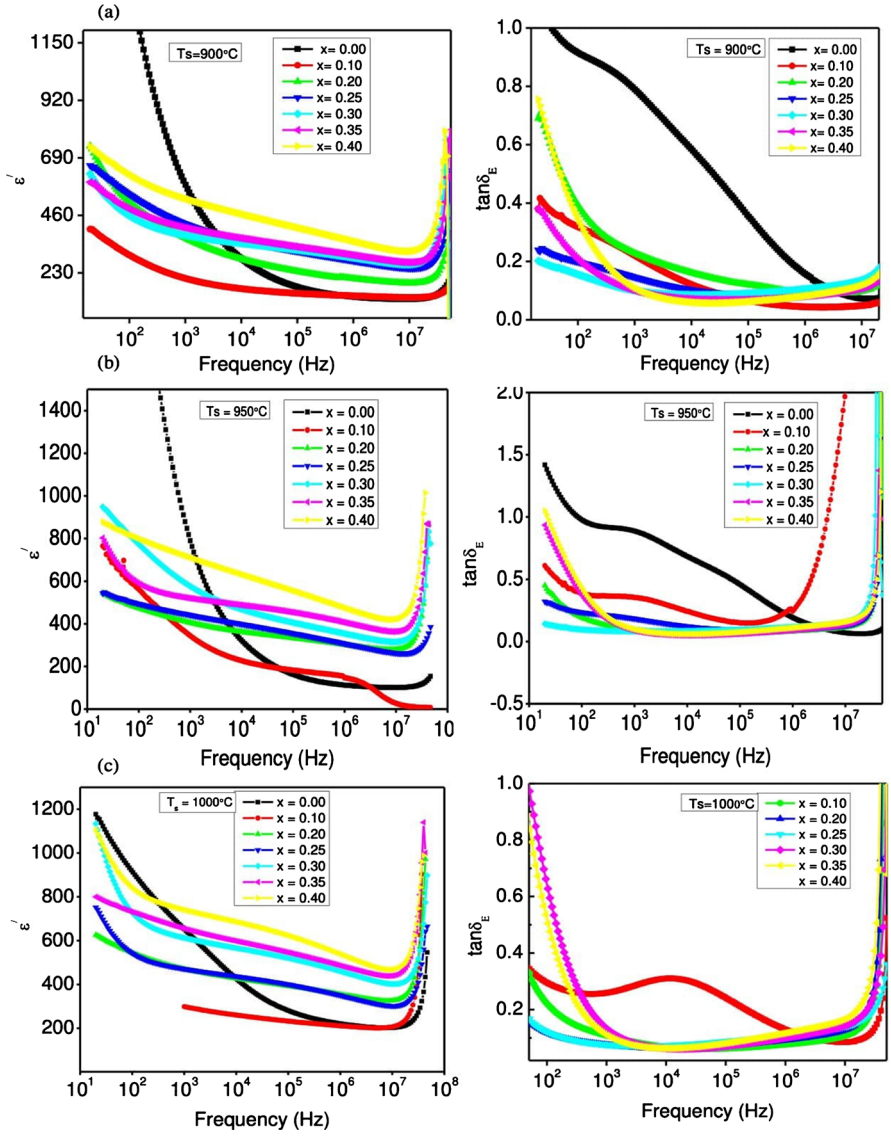

Figure 5. Variation of dielectric constant, ε' and dielectric loss ($\tan\delta$) of various xBST-(1 − x)BFGO ceramics sintered at (a) 900˚C, (b) 950˚C and (c) 1000˚C for 1 h.

potential energy by creating a polarization of electric charges in the dielectric material. The imaginary part of the dielectric constant represents the dielectric loss [16]. The variation of ε' with frequency can be written according to Debye equation as follows [17]:

$$\varepsilon' = \varepsilon_0 + \frac{\varepsilon_0 - \varepsilon_\infty}{1+\omega^2\tau^2}$$

where, τ^2 is the relaxation time, ε_∞ is the dielectric constant at a very high frequency and ε_0 is the dielectric constant at a very low frequency, respectively. This Debye equation indicates that ε' decreases with increasing frequency and this is in agreement with the behavior of ε' as shown in **Figure 5** for all samples. Decreasing of ε' can also be explained on the basis of polarization mechanisms (electric dipole moment per unit volume). Four types of polariza-

tions are available in polycrystalline ceramics such as electronic, ionic, dipolar and interfacial. Below 10^6 Hz all types of polarizations are present and between 10^6 Hz to 10^{11} Hz the electric dipoles present in a material are unable to follow the field. Moreover, in polycrystalline compound ε' mainly comes from space charge polarization and at high frequency the contribution of space charges are found to be too low that the value of ε' decreases rapidly. **Figure 5** also shows the variation of dielectric loss ($\tan\delta_E$) with frequency. The physical significance of $\tan\delta_E$ is the energy dissipation of the material in the dielectric system. The high value of $\tan\delta_E$ at lower frequencies corresponds to high value of resistivity due to the contribution of grain boundaries. The high frequency region corresponds to a low value of resistivity due to the grains. Moreover, rapid decreases of $\tan\delta_E$ at low frequency region and frequency independent at high frequency region can be explained on the basis of nature of space charge polarization according to Maxwell and Wagner which is good agreement with Koop's phenomenological theory [18] [19] [20]. At low frequencies, the space charges are able to follow the variation of frequency with applied field but at high frequencies, they don't have enough time to build up and undergo relaxation. The low value of $\tan\delta_E$ at higher frequencies shows potential implementation of these materials in high frequency microwave devices, magnetically tunable filters, resonators and oscillators. Besides this, $\tan\delta_E$ depends on several factors, such as stoichiometry, structural homogeneity, composition behavior and sintering temperature of the samples [21].

Figure 6 shows the sintering temperature dependence of dielectric properties of various xBST-(1 – x)BFGO ceramics for a particular frequency (2 kHz). It is well known that the dielectric constant of ceramics mainly depends on grain size or particle size. It is a common fact that grain size is a very important parameter getting high dielectric constant. It is reported that samples have fine grain size consists of higher internal stress than the coarsely grained samples [22]. Density is also an important parameter in the process of polarization phenomenon. It is noticed that increases in density decreases the porosity resulting greater number

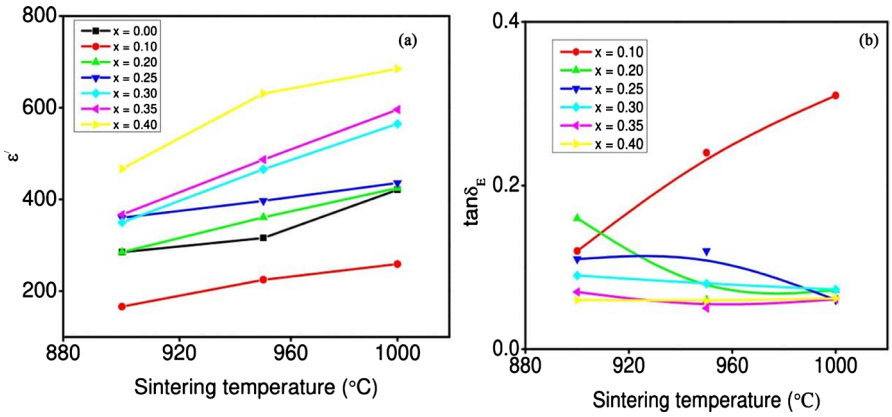

Figure 6. Comparison of temperature dependent (a) dielectric constant (ε') and (b) dielectric loss ($\tan\delta_E$) at three different sintering temperatures at a particular frequency.

of polarizing species per unit volume [23]. It is shown of **Figure 6(a)**, dielectric-constant (ε') of the prepared samples gradually increases with increasing sintering temperature from 900˚C to 1000˚C. **Figure 6(b)** shows the variation of dielectric loss ($\tan\delta_E$) with sintering temperatures (T_S) and it is reducing with the rise in T_S.

3.5. Complex Impedance Analysis

A polycrystalline material consists of grains and grain boundaries. Contribution of grains or grain boundaries in conduction mechanism of the compound can be separated by the complex impedance analysis. Equation of complex impedance is illustrated according to Debye model [24] as:

$$\begin{aligned} Z^*(\omega) &= Z' - jZ'' \\ &= \left[1/R + j\omega C\right]^{-1} \\ &= \left(R - j\omega R^2 C\right)/1+\left(\omega CR\right)^2 \\ &= \left[R/1+\left(\omega CR\right)^2\right] - j\left[R^2\omega C/1+\left(\omega CR\right)^2\right] \end{aligned}$$

where, $Z' = R/\left[1+\left(\omega CR\right)^2\right]$ and $Z'' = R^2\omega C/\left[1+\left(\omega CR\right)^2\right]$.

Z' is the real and Z'' is the imaginary part of complex impedance Z^*.

Figures 7(a)-(c) show the Nyquist plot (Z' vs. Z'' plot) of various xBST-(1 − x)BFGO ceramics in a wide range of frequency sintered at three different temperatures. All plots display a single depressed semicircular arc which are fitted with an equivalent circuit (RQC) built up of a resistance, capacitance and constant

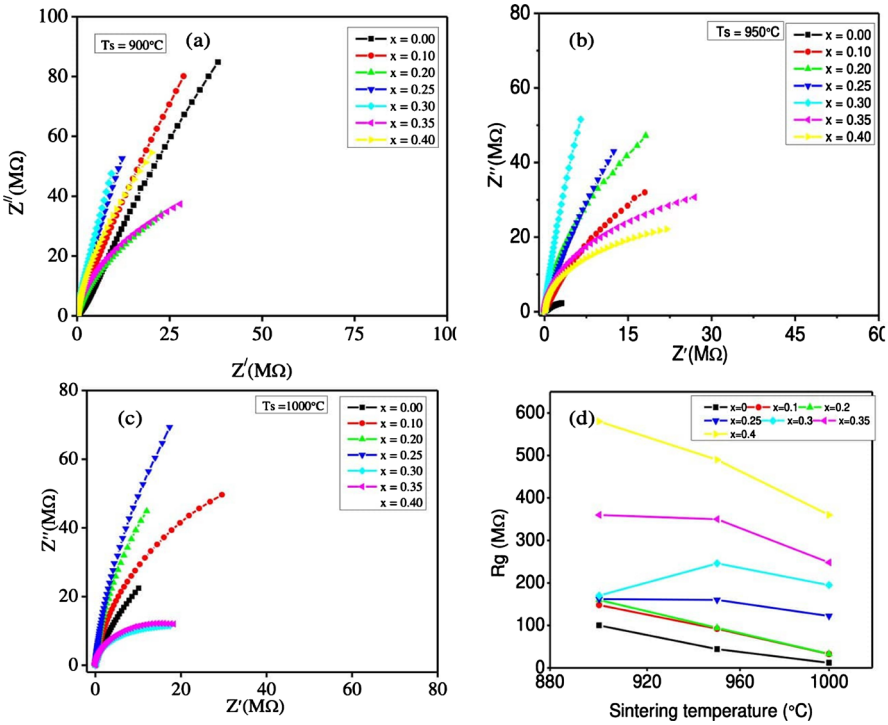

Figure 7. Nyquist plots of the xBST-(1 − x)BFGO samples sintered at (a) 900˚C, (b) 950˚C, (c) 1000˚C & (d) comparison of grain resistance for three different sintering temperatures.

phase element (Q) cascaded parallel to each other. According to brick-layer model [25] a semicircle creation in the total impedance of Z' vs. Z'' plot of polycrystalline ceramics indicates grain effects, second semicircle indicates grain boundary effects and third one indicates the presence of electrode effects. Homogeneous (ideal) samples generally follow the Debye behavior (*i.e.* formation of a perfect semicircular arc with the center on the real axis) [26]. However, contribution of grains is found to be dominated for the case of prepared samples because all samples exhibit a single semicircular arc with an initiation of second one.

Grain resistance (resistance due to grains, R_g) is determined form the Z' vs. Z'' plot. It is the value of resistance where the semicircular arc is coincided along X-axis of Z' vs. Z'' plot. The resistance in the equivalent circuit expresses the conductive path and the capacitance expresses the space charge polarization region. **Figure 7(d)** exhibits the variation of grain resistance (R_g) with the sintering temperature and it is found to be reduced with the rise in sintering temperature.

4. Discussion of the Observations

The studied compound is synthesized using solid state reaction technique. There are several techniques to prepare ceramic materials such as co-precipitation, solid state reaction technique, organic precursors, sol-gel synthesis, combustion synthesis etc. Now a day, the majority of ceramic powders are made by the standard solid state reaction technique and it is known as conventional ceramic process. This process has various advantages compare to others. Raw materials used for this technique are available in the market and the product can be prepared easily. Moreover, it is a cost effective technique because raw materials used for this technique is much chipper than other methods. The effect of sintering temperature on density, complex initial permeability, dielectric properties and impedance characteristics of the prepared material is illustrated in the above section and discussion of the observations are mentioned below.

It is noticed that the lattice constant (a) and the volume (V) are slightly increase for the sample sintered at 950˚C which indicates the expansion of the unit cell and thereby a probability of improved permeability may be observed. On the other hand, the value of a and V decrease after 950˚C which may be due to the creation of some oxygen vacancies for higher temperature sintered samples [26]. Sintering at high temperature leads to accelerate the grain which causes to reduce pores in the samples [27]. Existence of low amount pores in the samples indicates the grains are tightly concentrated and make them close to each other which help to increase the values of ρ_B with increasing sintering temperatures.

The value of μ' increases up to 950˚C is related to density because the increase in density leads to decrease in porosity, which reduces the demagnetizing field due to the pores [28]. The reduction of μ' above 950˚C may be due to their high sintering temperature which creates some pores inside the grains. The

porosity in ceramic materials is of two types: intergranular porosity and intra-granular porosity. Thus, the total porosity (P) can be written as, $P = P_{inter} + P_{intra}$. The major obstacle originates in a material from the intergranular type porosity and this type of porosity arises when a compound is melted or damaged due to sintering at high temperature. On the other hand, intra-granular type porosity may take place in a substance during sintering at any temperature. The value of μ' for the prepared samples sintered above 950˚C is found to be decreased and this might be attributed to the presence of intra-granular type porosity because the intra-granular type porosity resists the movement of domain walls.

The value of ε' is found to be increased with the increase in sintering temperature and this expected enhancement can be explained on the basis of density and grain size. Density of the samples increases with increasing sintering temperature (**Figure 2**) and fine grains are expected with the rise in sintering temperature and these might be attributed to obtain high value of ε'. The value of $\tan\delta_E$ decreases with increasing sintering temperature. This is due to the activeness of grain at higher temperature which means low amount of energy is required to transfer electron from one grain to others. It is observed that with the rise in sintering temperature the radius of the semicircular arcs reduces resulting in a decrease of effective resistance (grain resistance, R_g) and increase of motion of electrons within a grain. Electrons in a bigger size grain get more space to move than a smaller size grain. Bigger size grains are expected for the prepared compound during the rise of sintering temperature as a result conduction of electrons within a grain might be accelerated.

5. Conclusion

The effect of sintering temperature (900˚C, 950˚C and 1000˚C) on density, complex initial permeability, dielectric properties and impedance analysis of $xBa_{0.95}Sr_{0.05}TiO_3$-$(1-x)BiFe_{0.90}Gd_{0.10}O_3$ ceramics were studied. The polycrystalline ceramics were fabricated by conventional solid state reaction method. X-ray diffraction pattern indicated that the crystal structure of the ceramics was cubic and sintering temperature did not affect the structure but the volume of the unit cell changed due to creation of oxygen vacancies. Density of the compositions increased with the increase in sintering temperature which is common phenomenon of the activeness of grain at higher temperature. Incorporation of BST into BFGO improved magnetic properties (complex initial permeability) at room temperature. It was also observed that 950˚C sintering temperature is more favorable getting better magnetic properties for the prepared ceramics. On the other hand, comparatively better dielectric properties were obtained for 1000˚C sintering temperature. Moreover, with the increase in sintering temperature the radius of the semicircular arcs in the Nyquist plot (Z' vs. Z'' plot) decreased suggesting a decrease in effective resistance. In the conduction process of the studied samples majority of conduction due to grains was noticed. The studied ceramics is a lead-free compound and it can be used as an environment friendly material.

Acknowledgements

The authors greatly acknowledge the authority of Comilla University, Bangladesh to provide financial support for this research.

Conflicts of Interest

The authors declare no conflicts of interest regarding the publication of this paper.

References

[1] Barsoum, M.W. (2002) Fundamental of Ceramics. Taylor & Francis, Abingdon.

[2] Sunder, V., Halliyal, A. and Umarji, A.M. (1995) Investigation of Tetragonal Distortion in the $PbTiO_3$-$BiFeO_3$ system by High-Temperature X-Ray Diffraction. *Journal of Materials Research*, **10**, 1301-1306. https://doi.org/10.1557/JMR.1995.1301

[3] Shariq, M., Kaur, D. and Chandel, V.S., (2016) Investigation of Structural and Magnetic Properties of Pb Free Multiferroic $(BiFeO_3)_{(1-x)}$-$(BaTiO_3)_x$ Solid Solutions. *AIP Conference Proceedings*, **1742**, Article ID: 030018.

[4] Smith, R.T., Achenbach, F.D., Gerson, R. and James W.J. (1968) Dielectric Properties of Solid Solutions of $BiFeO_3$ with Pb(Ti, Zr)O_3 at High Temperature and High Frequency. *Journal of Applied Physics*, **39**, 70-74.

[5] Kumer, M., Srinivas, A., Suryanarayana, S.V. and Bhimasankaram, T. (1998) Dielectric and Impedance Studies on $BiFeO_3$-$BaTiO_3$ Solid Solutions. *Physica Status Solidi* (*A*), **165**, 317-326. https://doi.org/10.1002/(SICI)1521-396X(199801)165:1%3C317::AID-PSSA317%3E3.0.CO;2-Y

[6] Cai, W., Zhong, S.X., Fu, C.L., Chen, G. and Deng, X.L. (2014) Microstructure, Dielectric and Ferroelectric Properties of $xBaZr_{0.2}Ti_{0.8}O_3$-$(1-x)BiFeO_3$ Solid Solution Ceramics. *Materials Research Bulletin*, **50**, 259-267. https://doi.org/10.1016/j.materresbull.2013.11.029

[7] Miah, M.J., Khan, M.N.I. and Akther Hossain, A.K.M. (2016) Weak Ferromagnetism and Magnetoelectric Effect in Multiferroic $xBa_{0.95}Sr_{0.05}TiO_3$-$(1-x)BiFe_{0.9}Gd_{0.1}O_3$ Relaxors. *Journal of Magnetism and Magnetic Materials*, **401**, 600-611. https://doi.org/10.1016/j.jmmm.2015.10.083

[8] Ahad, A, Taher, M.A., Das, M.K., Rahaman, M. Zahidur and Khan, M.N.I. (2019) Effect of Y Substitution on Magnetic and Transport Properties of $Ba_{0.95}La_{0.05}Ti_{1-x}Y_xO_3$ Ceramics. *Results in Physics*, **12**, 1925-1932. https://doi.org/10.1016/j.rinp.2019.01.072

[9] Miah, M.J., Khan, M.N.I. and Akther Hossain, A.K.M. (2016) Synthesis and Enhancement of Multiferroic Properties of $(x)Ba_{0.95}Sr_{0.05}TiO_3$-$(1-x)BiFe_{0.90}Dy_{0.10}O_3$ Ceramics. *Journal of Magnetism and Magnetic Materials*, **397**, 39-50. https://doi.org/10.1016/j.jmmm.2015.08.079

[10] Angadi, V.J., Rudraswamy, B., Sadhana, K. and Praveena, K. (2016) Structural and Magnetic Properties of Manganese Zinc Ferrite Nanoparticles Prepared by Solution Combustion Method Using Mixture of Fuels. *Journal of Magnetism and Magnetic Materials*, **409**, 111-115. https://doi.org/10.1016/j.jmmm.2016.02.096

[11] Smit, J. and Wijn, H.P.J. (1959) Ferrites, Chap. XIII. Cleaver Hume Press Ltd., London.

[12] Akther Hossain, A.K.M., Khirul Kabir, K., Seki, M., Kawai, T. and Tabat, H. (2007)

Structural, AC, and DC Magnetic Properties of $Zn_{1-x}Co_xFe_2O_4$. *Journal of Physics and Chemistry of Solids*, **68**, 1933-1939.

[13] Verma, A. and Chatterjee, R. (2006) Effect of Zinc Concentration on the Structural, Electrical and Magnetic Properties of Mixed Mn-Zn and Ni-Zn Ferrites Synthesized by the Citrate Precursor Technique. *Journal of Magnetism and Magnetic Materials*, **306**, 313-320. https://doi.org/10.1016/j.jmmm.2006.03.033

[14] Cullity, B.D. and Graham, C.D. (2008) Introduction to Magnetic Materials. 2nd Edition, John Wiley & Sons, Hoboken. https://doi.org/10.1002/9780470386323

[15] Verma, A, Goel, T.C. and Mendiratta, R.G. (2000) Frequency Variation of Initial Permeability of NiZn Ferrites Prepared by the Citrate Precursor Method. *Journal of Magnetism and Magnetic Materials*, **210**, 274-278. https://doi.org/10.1016/S0304-8853(99)00451-5

[16] Zhi, J., Chen, A., Zhi, Y., Vilarinho, P.M. and Baptista, J.L. (2004) Incorporation of Yttrium in Barium Titanate Ceramics. *Journal of the American Ceramic Society*, **82**, 1345-1348. https://doi.org/10.1111/j.1151-2916.1999.tb01921.x

[17] Kingery, W.D., Bowen, H.K. and Uhlman, D.R. (1976) Introduction to Ceramics. 2nd Edition, Wiley Interscience, New York.

[18] Maxwell, J.C. (1873) Treatise on Electricity and Magnetism. 1st Edition, Clarendon Press, Oxford.

[19] Wagner, K.W. (1913) Zur Theorieder Unvolkommenen Dielektrika. *Annalen der Physik*, **345**, 817-855. https://doi.org/10.1002/andp.19133450502

[20] Koops, C.G. (1951) On the Dispersion of Resistivity and Dielectric Constant of Some Semiconductors at Audio Frequencies. *Physical Review*, **83**, 121-124. https://doi.org/10.1103/PhysRev.83.121

[21] Devan, R. and Sand Chougule B.K. (2007) Effect of Composition on coupled Electric, Magnetic, and Dielectric Properties of Two-Phase Particulate Magnetoelectric Composite. *Journal of Applied Physics*, **101**, Article ID: 014109. https://doi.org/10.1063/1.2404773

[22] Shrivastav, B.D., Barde, R., Mishra, A. and Phadake, S. (2013) Dielectric Behavior of Biomaterials at Different Frequencies on Room Temperature. *Journal of Physics: Conference Series*, **534**, Article ID: 012063. https://doi.org/10.1088/1742-6596/534/1/012063

[23] Thangjam, B. and Soibam, I. (2017) Comparative Study of Structural, Electrical and Magnetic Behaviour of Ni-nCu-Zn Nanoferrites Sintered by Microwave and Conventional Techniques. *Journal of Nanomaterials*, **10**, Article ID: 5756197. https://doi.org/10.1155/2017/5756197

[24] Cao, W. and Gerhardt, R. (1990) Calculation of Various Relaxation Times and Conductivity for a Single Dielectric Relaxation Process. Solid State Ion, **42**, 213-221. https://doi.org/10.1016/0167-2738(90)90010-O

[25] MacDonald, J.R. (1987) Impedance Spectroscopy. Wiley-Interscience, New York.

[26] Sahoo, S., Mahapatra, P.K. and Choudhary, R.N.P. (2016) Effect of Sintering Temperature on Dielectric, Electrical and Magneto-Electric Characteristics of Chemico-Thermally Synthesized $(Ba_{0.9}Gd_{0.1})(Ti_{0.9}Fe_{0.1})O_3$. *Ceramics International*, **42**, 15955-15967.

[27] Ahmad, S.I., Rao, P.K. and Syed, I.A. (2016) Sintering Temperature Effect on Density, Structural and Morphological Properties of Mg- and Sr-Doped Ceria. *Journal of Taibah University for Science*, **10**, 381-385. https://doi.org/10.1016/j.jtusci.2015.04.003

[28] Dimri, M.C., Verma, A., Kashyap, S.C., Dube, D.C., Thakur, O.P. and Prakash, C. (2006) Structural, Dielectric and Magnetic Properties of NiCuZn Ferrite Grown by Citrate Precursor Method. *Materials Science and Engineering B*, **133**, 42-48. https://doi.org/10.1016/j.mseb.2006.04.043